Removal of Pb(II) ions from solution using chemically modified *Luffa cylindrica* as a method of sustainable water treatment

Akanimo U. Emene, Robert Edyvean

Abstract: *Luffa cylindrica*, readily available in parts of Asia, Africa and South America, when chemically treated with 4% NaOH shows an increased amount of ion exchange functionality, thereby enhancing the adsorption capacity. It is well known for loofa sponge production and it is regarded as a common waste material. Chemical modification of *Luffa cylindrica* also changes its structural characteristics by exposing its pores for enhanced adsorption and shows an increased BET surface area from 25.32 m^2/g to 43.10m^2/g. From the FT-IR spectra an increase in protonated hydroxyl and carboxyl functional groups was observed. The adsorption of Pb^{2+} onto alkali treated *Luffa cylindrica* (ATLC) was investigated in batch experiments as a function of pH, temperature, initial metal ion concentration and ionic strength. The ATLC was found to be the more effective in removing Pb^{2+} from aqueous solution as compared to the neutral treated *Luffa cylindrica*. Adsorption kinetic and isotherm models, pseudo second order, Langmuir, two-site Langmuir, Dubinin-Radushkevich and Sips were utilized in understanding the adsorption mechanism and the ability of the adsorption system evaluated. The maximum adsorption capacity is 24.9mg/g as described by the Langmuir isotherm and the maximum percentage uptake (efficiency) is 96.4%. The Sips model fits better than the Langmuir, two site Langmuir and Dubinin-Radushkevich model using GraphPad. The kinetics of the biosorption process was studied. A pseudo second order model shows a good correlation fit.

Keywords: Biosorption, ion exchange, lead, *Luffa cylindrica (L. cylindrica)*, Alkali treated *Luffa cylindrica* (*ATLC*).

1 Introduction

Lead is a heavy metal pollutant that contaminates water and soil environments. It is a global problem, affecting most industrialised nations, as well as developing nations [1]. The release of lead into the environment, and its subsequent uptake by plants and animals causes serious health problems and environment issues. It is a major health risk, particularly in developing countries [2].

The prominence of environmental lead contamination results both from its persistence [3], [4], [5] and from its present and past numerous sources. Sources of lead contamination are typically anthropogenic: fuel burning (particularly incomplete combustion from vehicles), mining operations, lead-based paints, tyre wear, electroplating activities, plastic, smelting, paper manufacturing industries, pesticides, leakage of oils, metal mining and corrosion of batteries and metallic parts such as radiators, etc. [1],[6],[7] . Lead contamination of surface waters is a particular problem in Nigeria: Leaching of lead pipes, run off from roads and extensive utilization of crude oil have resulted in wide spread contamination [8]. The major source of contamination in Nigeria is from the large scale production, transport and disposal of petroleum products [9]. Oil exploration in the Niger Delta (South of Nigeria) has been ongoing for decades and the United Nations Environment Programme (UNEP) have set targets for clean-up and remediation of the area. Furthermore, poor industrial practice has resulted in some pharmaceutical companies in Nigeria discharging effluents that contain concentrations of lead above the WHO recommended maximum contaminant concentration level [10].

Lead has no known biological function in living organisms. If ingested or inhaled, lead and its compounds are poisonous to animals and humans. Lead is a neurotoxin that accumulates both in soft tissues and in bones, damaging the nervous system and causing brain disorders. Excessive lead also causes blood disorders in mammals [2].The maximum recommended safe daily intake, biomarker for lead toxicity, for humans is as low as 1.0 μg/g. Lead is also highly toxic to plants, restricting root elongation and plant growth, and impairs transpiration and chlorophyll production [11].

As the largest and fastest growing economy in Africa, Nigeria is expected to lead by example and engage in the global drive to tackle environmental contamination and enhance the sustainability of the environment [12]. With its rapid industrialization and population growth, it is critical for Nigeria to ensure that the effective treatment of wastewater is prioritised to reduce environmental and health impacts of contaminated waterways, and the subsequent negative impact on the socio-economic development of the country [1].

Studies carried out on the treatment of heavy metal pollution in wastewater have highlighted a pressing need to develop low cost, environmentally friendly and effective materials to tackle this issue [1],[13].

Biosorbents are biological materials with functionalised surfaces capable of removing trace metals and other contaminants from water. These materials are favoured for their renewable nature, and their ability to biodegrade. Current research has focused on plant materials that are by-products of other industries, such as sawdust, coconut husks or palm kernel shells [14],[15]. Also of interest are plants that grow easily in, and are well suited to, the conditions found in the community that will actually make use of the biosorbent technology.

The loofa sponge, derived from the sub-tropical plant *Luffa cylindrica (LC),* is grown annually in China, Japan, Nigeria and many countries in South America. In Nigeria, the loofa fruit is commonly grown as a feed for poultry and as a vitamin supplement for aqua feeds. The fibrous residue of the fruit (mature fruit) is used in producing gourds and loofa sponges, after which it is regarded as a waste material [15]. The smooth and cylindrical shaped fruit is about 12cm long, the flesh of which is a sponge-like material that is comprised of a reticulate matrix consisting of various fibrous interwoven cords. The cellular structure of the cords is made up parenchyma cells that are responsible for the metabolic activities of the plant. The network of these cords comprises flexible and hollow cylindrical fibres [16],[17]. These cords are composed of fibrils which are resinous lignocellulose material comprising of 55-90% cellulose, 10-23% lignin, 8-22% hemicellulose (the exact proportions depending on factors such as plant origin, weather conditions, nature of soil, etc.) [18]. It is this inner part of the fruit which, when dried, forms the typical loofa sponge that has been employed for centuries as a sponge or scrubber for washing.

The high proportion of cellulose material in *LC* can be utilised in the removal of heavy metal ions from aqueous solution due to the presence of active functional groups within the molecular structure. Studies have shown that the *LC* material is able to remove both metal cations [6], [19] and organic pollutants from aqueous solutions. Furthermore, due to the type of functional groups present in the cellulosic structure, *LC* can be chemically modified to enhance its sorption properties [20],[21]. Suhas *et al.*[22], modified cellulose, which is a dominant material of *LC*, by chemicals to enhance the adsorption capacity of metal ions and this is attributed to an increase in the surface area as well as more accessible functional groups for adsorption [22]. Treatment with acids and alkali has been widely used to enhance the sorption properties of biomaterials. *LC* has also been utilised as an immobilising medium to provide reliable support for the immobilisation of microalgae for the removal of toxic metal ions from wastewater [23].

LC represents a low cost, renewable, biodegradable solution for sustainable water treatment in Nigeria [24]. However, before it can be developed as a viable, large-scale process, it is necessary to gain a thorough understanding of the chemistry involved, so that the process can be optimized. This requires

an understanding of the chemistry of the wastewater streams, the surface properties of *LC*, and the metal surface complexes formed during removal of lead from water.

Here, we investigate the efficiency of AT*LC* as an adsorbent in the removal of Pb (II) ions from aqueous solution, across the pH range 3-9. The methodology used to modify the *LC* requires little energy and presents a promising optimization strategy for a developing country like Nigeria. The results obtained contribute to the understanding of the surface properties of *LC*, as well as the *LC*-Pb biosorption mechanism.

2 Material and methods

2.1 Reagents and stock solutions

All chemicals utilised were of analytical grade. The stock solution, 1 g/L of Pb (II) was prepared by dissolving $PbCl_2$ salt, obtained from Sigma-Aldrich, United Kingdom, in deionised water. The desired concentrations were obtained by diluting the stock solution to set concentrations, varied from 50 to 200mg/L. 0.1 M HCl and NaOH solutions were used to alter the solution pH.

2.2 Chemical Modification of *Luffa Cylindrica (LC)*

Dried fruit of *LC* were purchased commercially in the United Kingdom. The pale yellow *cylindrica* fibre were washed several times with distilled water to remove surface impurities and seeds, then alkali treated by soaking in 4% NaOH at room temperature for 1h. It was repeatedly washed in distilled water until the pH was almost neutral, and then oven dried at 90 °C for 24h.The dried samples were ground and sieved to a 1 mm particle size fraction and stored for utilization in further experiments. The treatment of *LC* is regarded as a surface clean up and preparation process [23].

2.3 Characterisation of AT*LC*

2.3.1 Surface Analysis of ATLC and LC

The surface structure of loofa was analysed by an Analytical Scanning Electron Microscope (SEM) (Model JOEL JSM- 6010LA) coupled with energy dispersive X-ray (EDX) with an accelerating voltage of 10kV and at a magnification of x550 SS60. The chemical characteristics was analysed by using a Nicolet 6700 Fourier Transform Infra-red (FT-IR) Spectrometer to identify the functionality that interacts with lead ions. 50mg of dried *ATLC* (< 250μm thickness) were prepared for ATR- FTIR analysis. Measurements were made in transmittance mode using a spectral resolution of $4cm^{-1}$ by 256 scans and approximately 150 seconds per step across the range $4000cm^{-1}$ to 650 cm^{-1}. The surface area of each sample of loofa was determined from nitrogen adsorption at 77.2K in the range of relative pressure (p/p^0) of 0.05 – 1 by using a Micromeritics 3Flex instrument. The samples were degassed at 150°C for 24 hours. A three-parameter non-linear fitting procedure was used and the loofa samples were subjected to a 99-point BET surface analysis and a full adsorption isotherms were collected for all samples. The conventional single point method of relative pressure was used.

2.3.2 Zeta potential measurements

The electrophoretic mobility technique was conducted to measure the zeta potential by using a Malvern Zetasizer Nano Instrument. 0.1% concentration of *ATLC* in 0.01mol/L NaCl aqueous solution was stirred continuously with a magnetic stirrer. As desired, the pH was adjusted by addition of 0.1M of HCl and 0.1M NaOH over a range of pH 2-10. The pH of the sample solution was measured before each measurement. The samples were loaded into a capillary cell and measurements were performed at room temperature (21°C). An average of three measurements were recorded for each analysed sample [25],[26].

2.3.3 Ion exchange loading capacity

A single contact of 1g of 1mm sieve size *ATLC* was mixed with 100 mL of aqueous simulant feed of 0.1M NaOH using a magnetic stirrer for 24hrs. Then the filtered sample was rinsed off with distilled water until neutral pH and then contacted with 100ml of aqueous solution of 0.1M HCl and mixed for 24hrs. After which the filtered sample was used for further batch adsorption experiments. The filtered *ATLC* from step 1 was mixed with 1M NaCl for 24hrs, sufficient time for exchange of ions in the solution. Then the filtrate solution obtained, after the contact time of exchange of ions, was titrated against 0.1M NaOH. The pH was then recorded at each point [27].

2.4 Batch adsorption experiments

All batch studies as a function of acid concentration were carried out as single contacts with the contact of 1g of 1mm sieve size 4% alkali treated *Luffa cylindrica* (*ATLC*) with 200 mL of aqueous solution. Experiments were carried out at Pb (II) concentrations of 50, 70,100, 150 and 200mg/L; and each at pH 3, 5, 7 and 9 at 50mg/L. The *ATLC* and aqueous solution were continuously mixed at an agitation speed of 200rpm for a period of 24 hrs at room temperature (21 °C) on a magnetic stirrer. Distribution behaviour was determined using the following;

$$q_e = \left(\frac{C_i - C_e}{C_e}\right) \times \frac{v}{m} \quad (1)$$

q_e is the weighted distribution of the metal ions where C_i is the initial aqueous concentration of the metal ions before contact and C_e is the aqueous concentration of the metal ions after equilibration. V is the volume of the aqueous phase (mL) and m is the mass of the *ATLC* (g). The percentage removal (R%) was determined by difference (using (2)) and the concentrations of the lead determined by ICP-MS.

$$R\% = \frac{C_i - C_e}{C_i} \times 100 \quad (2)$$

Where C_i is the initial metal concentration before contact and C_e is the concentration of the metal ion in the aqueous phase after contact with the *ATLC*. pH measurements for solutions were determined using a silver/silver chloride reference electrode calibrated from pH 4-7 using buffers. Error was determined by triplicate measurement in aqueous solution concentrations prior to contact.

2.5 Ionic strength effect

All batch experiments were carried out as single contacts with the contact of 250mg of 1 mm sieve size *ATLC* with 50ml of both NaCl (0.1 M, 0.5 M and 1 M) and 50 mg/L lead chloride solution (100 mg/L Cl^-). The *ATLC* and binary solution were continuously mixed at an agitation speed of 200rpm for a period of 24hrs at pH 5 at room temperature (21°C) on a magnetic stirrer. The distribution behaviour and percentage removal were determined using equation (1) and (2) and the concentrations of both lead and sodium ions were analysed by ICP-MS.

2.6 Determination of loading behaviour.

All loading isotherms were carried out as single contacts with the contact of 1 g of *ATLC* with 200 mL of aqueous solution. The *ATLC* and aqueous solution were continuously mixed at an agitation speed of 200rpm for a period of 24 hrs at room temperature (21°C). A widely researched and commonly used two parameter fitting model, was used to determine the fitting ability due to its quantitative criteria for evaluation [28],[29]. The 3 parameter model which gives a clearer evaluation of the data was also utilised. The data were fitted to Langmuir, two site Langmuir, and Dubinin-Radushkevich [28] and Sips models, equations (3-8).

2.7 Calculations

The fitting was carried out by using linear regression and by non-linear least squares analysis using GraphPad [28].

Langmuir

$$q_e = \frac{K_L C_e}{1+a_L C_e} \quad (3)$$

The monolayer saturation capacity, q_m (mg L^{-1}), was calculated from the Langmuir equation using equation (4).

$$K_L = q_m a_L \quad (4)$$

Dubinin-Radushkevich

$$q_e = q_D \exp(-B_D \left[RTln\left(1+\frac{1}{C_e}\right)\right]^2) \quad (5)$$

Where the mean free energy of sorption, E, can be calculated using B_D in equation (6).

$$E = \frac{1}{\sqrt{2B_D}} \quad (6)$$

Two site Langmuir

$$q_e = \frac{Q_1 b_1 C_e}{1+b_1 C_e} + \frac{Q_2 b_2 C_e}{1+b_2 C_e} \quad (7)$$

Sips

$$q_e = \frac{K_S C_e^{\beta s}}{1+a_s C_e^{\beta s}} \quad (8)$$

Error in the isotherm constants was calculated from the linearized form of the model using the EXCEL calculated values using the deviations of the experimental data from this best fit line.

2.8 Determination of the kinetics of extraction

Batch kinetics was carried out with the contact of 1 g of *ATLC* with 200 mL of aqueous simulant feed. The *ATLC* and aqueous feed were continuously mixed for a period of 24 hrs at 21 °C and 5 mL samples were extracted at set time intervals. The data was fitted using a linear fit of pseudo second order models, which do not take into account the mechanism of reaction.

The linear form of the pseudo-second-order kinetic model [30] is as follows;

$$\frac{t}{q_t} = \frac{1}{k_2 {q_e}^2} + \frac{1}{q_e} t \quad (9)$$

Where k_2 = pseudo second order reaction constant (hr^{-1}). The non-linear form for the pseudo second-order kinetics is given below:

$$q_t = \frac{k_2 q_e^2 t}{1+k_2 q_e t} \quad (10)$$

The non-linear form was fitted using the minimization of the sum of square errors (SSE) using SOLVER [31]. The $t_{1/2}$ was calculated by the relationship;

$$t_{1/2} = \frac{1}{k_2 q_e} \quad (11)$$

The initial sorption rate h_0 (30) is given by;

$$h_0 = k q_e^{\,2} \quad (12)$$

3 Results and Discussion

3.1 Chemical modification of *Luffa cylindrica* (*LC*)

The morphology of *LC*, shown in Fig 1, appears dry and flaky with many loose particles on the surface. In Fig 2, the morphology of the NaOH treated loofa (*ATLC*) is more broken up with fewer loose particles on the surface. This may be as a result of exposure of the pores and removal of the lignin and hemicellulose compounds [32]. Ghali *et al*. [33] showed that treating *L. cylindrica* fibres with 4 % NaOH leads to a higher crystallinity index and to the improvement in adhesion capacity [33].

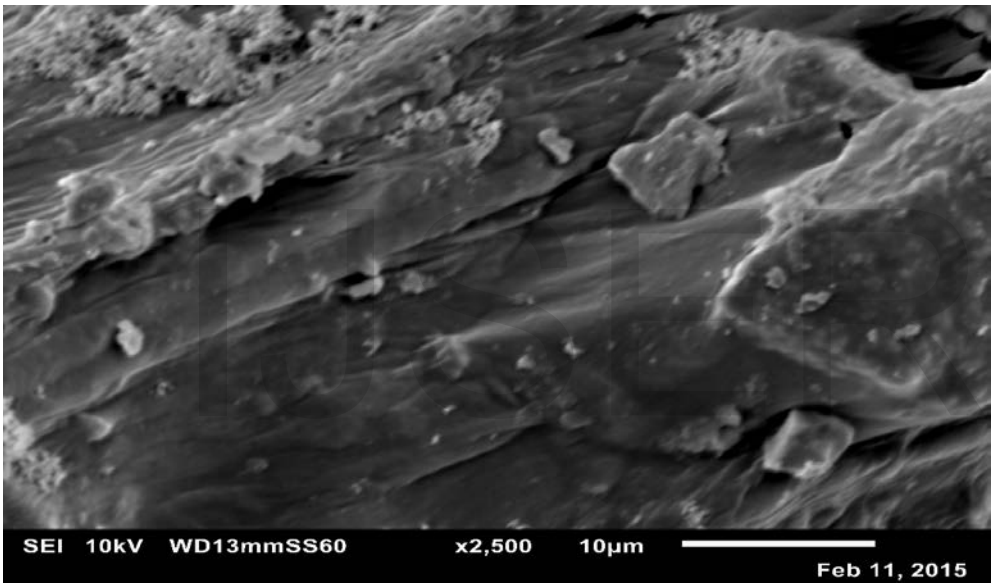

Fig. 1. Surface morphology of untreated loofa (raw loofa) by Emene

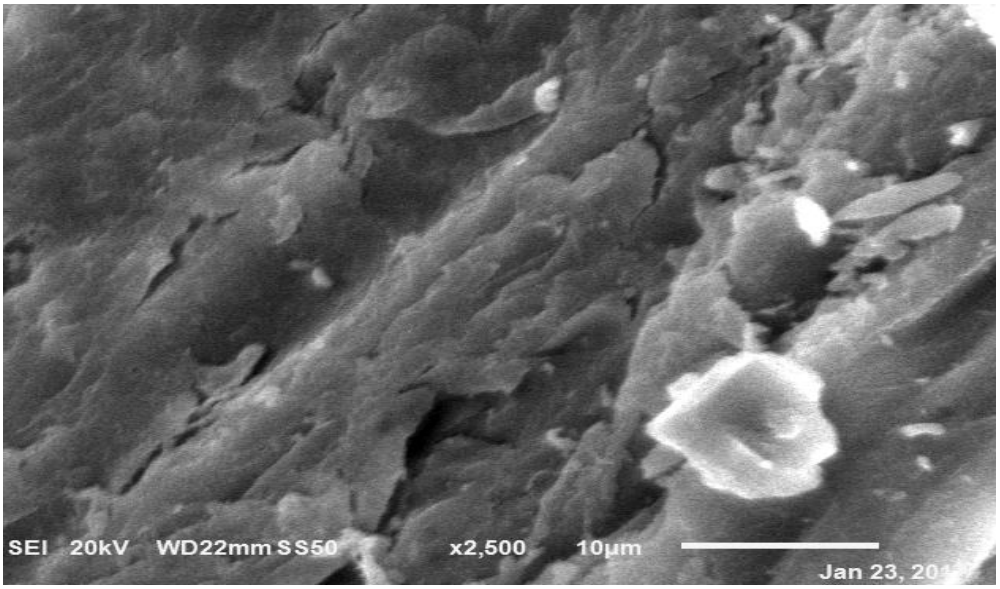

Fig. 2. Surface morphology of treated loofa (4% NaOH) by Emene

Alkali treatment has been used to enhance the properties of the *L. cylindrica* surface (33). The maximum percentage of NaOH to treat *L. cylindrica*, without damage to the crystalline region is reported to be 8%. Ghali *et al*. [33], investigated the pre-treatment of Luffa fibres by 4% NaOH that led to successful delignification (33). Modification of *L. cylindrica* with 4% NaOH bestows additional functionality of OH^- groups added onto the surface area of *L. cylindrica* [34], [35]. The higher the pKa (deprotonation constant) the greater the adsorption preference on the *ATLC* surface [33].

The surface characteristics of the NaOH treated loofa with a BET surface area of 43.096m^2/g is higher in value than the untreated at 25.322m^2 /g (see Table 1). This shows an increased surface area which accounts for the broken up and rougher loofa surface. The increase in surface area and pore volume after alkali treatment by 41.3% and 29.4% respectively shows the involvement of the loofa surface and particle pores in enhancing the adsorption process.

Table 1. BET result values of ATLC and untreated *L. cylindrica*

Data	Untreated	NaOH treated
Surface area	25.322 m^2/g	43.096 m^2/g
Specific surface area	5.748 m^2	6.995 m^2
Total pore volume	0.012 cm^3/g	0.017 cm^3/g

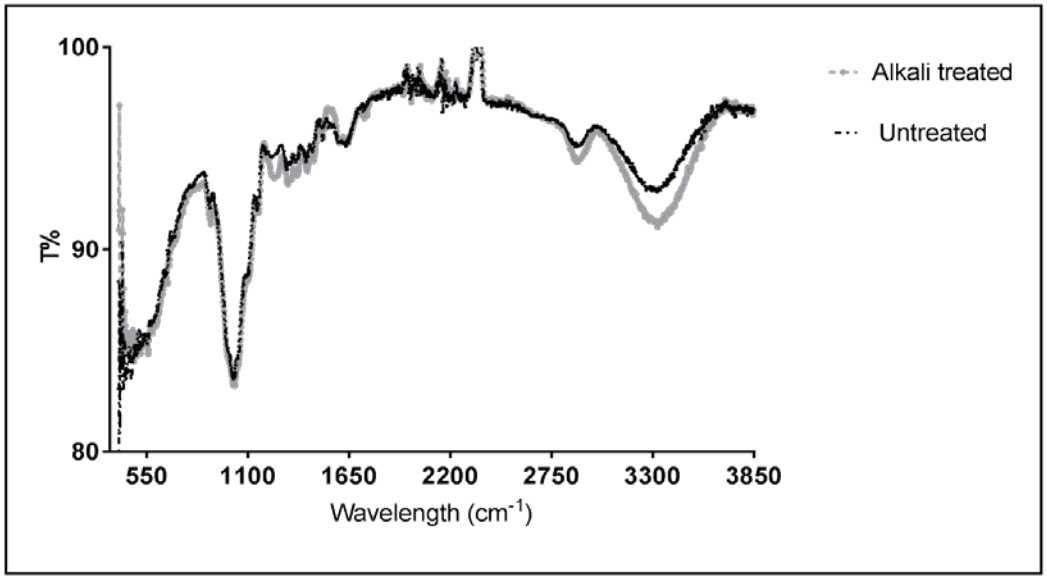

Fig. 3. FT-IR spectra of *ATLC* and untreated loofa at 21°C, 256 scans. T% represents Transmittance.

The change in the adsorption bands between untreated and treated loofa are shown in Fig 3 & 4. These indicate characteristic functional groups on the adsorbent and a change in the bands, across the range 800cm^{-1} to 4000cm^{-1}, and also a change in the surface chemistry of the *ATLC* following alkali treatment was observed at various points. The peak at 3340 cm^{-1} is attributed to the stretching vibration of the O-H group. A shift to 3323cm^{-1} and also to 1040cm^{-1}, including a decrease in peak intensity was observed, indicating a change in the binding energy pattern [21],[34],[36],[37]. The band stretching at 1035cm^{-1} and 1250cm^{-1} are attributed to the cellulose and the characteristic bands at 1450cm^{-1} to 1600cm^{-1} indicate lignin. An alteration of the peak at 1735cm^{-1} and 1550cm^{-1} are attributed to the disappearance of the hemicellulose and lignin contents [27],[38]. The majority characteristic adsorption bands are changed as shown in Table 2, which shows the effect of NaOH treatment focus on the various functional groups. The presence of a higher and stronger band at 3100cm^{-1} to 3600cm^{-1} may be as a result of the presence of exchangeable protons contained in the hydroxyl group which leaves room for adsorption to occur via ion exchange [39]. This stronger band exposes the hydroxyl groups for adsorption [36],[40]. The broad band in the range 3545-3050cm^{-1} indicates strong intramolecular hydrogen bonds that gives rise to strong adsorption [41],[42].

Table 2: Change in transmission FTIR results at specific regions of absorbance.

Region	ΔT%	Corresponding absorbance	Reference
1265cm^{-1}-1460cm^{-1} (fingerprint region)	+0.6 - +1.1	O-H bending	[43],[44]
1540cm^{-1}	-0.85	N-H bending	[45]
1735cm^{-1}	+0.6	C=O stretching (carbonyl group of ketone)	[43]
2890cm^{-1}	+0.8	C-H stretching	[21],[32]
3340cm^{-1}	+1.6	O-H bonding	[21],[36],[43]

On the other hand, NaOH treatment disrupts the hydrogen bonding of OH^- functional groups thereby ripping off H^+ for adsorption to occur [35],[46]. Carboxyl group are the dominant functional groups of *ATLC* in adsorption. Therefore, the difference in the binding energy of the functional groups as shown

by the spectra peaks indicates the importance of the role of O-H in the absorption of Pb^{2+} ions onto *ATLC* [47]. The characteristic bands that indicate the functional groups on the loofa surface show the structure of the loofa to possess lignin, cellulose and hemicellulose. Fig 4 shows an increase in the zeta potential values and an increase towards linearity when the loofa is treated with alkali. This change is explained by the change in the loofa structure after modification [48]. The untreated cucumber peel, a biosorbent material that contain cellulose, hemicellulose and lignin, which possess carboxyl and hydroxyl groups, also show a negatively charged surface that increases in zeta potential as the pH is increased (pH 2-6)[49]. Lower pH tends to cause the colloids in the system to coagulate and form more visible particles in solution. Therefore, the surface charge is expected to be lower at a lower zeta potential than at a higher zeta potential which occurs at a higher pH. The zeta potentials of *ATLC* over the pH range of 2 – 10 shows a negative surface charge on the loofa [50]**.** The increase in the magnitude of the negative zeta potential of *ATLC* shows the availability of free functional groups available for binding, which is responsible for the generated charge on the loofa surface [51]. The zeta potential increases as pH increases, which suggest a potential stability for lead adsorption as pH increases. The negative surface charge at increased pH to 8, explains the different factors that contribute to the uptake mechanism of metal ions onto loofa. Since formation of hydroxylated lead ions are expected over pH 6 (shown in Fig 7), pH 5 – 6 (optimum mV values) is determined as the appropriate pH for an effective adsorption process [52].

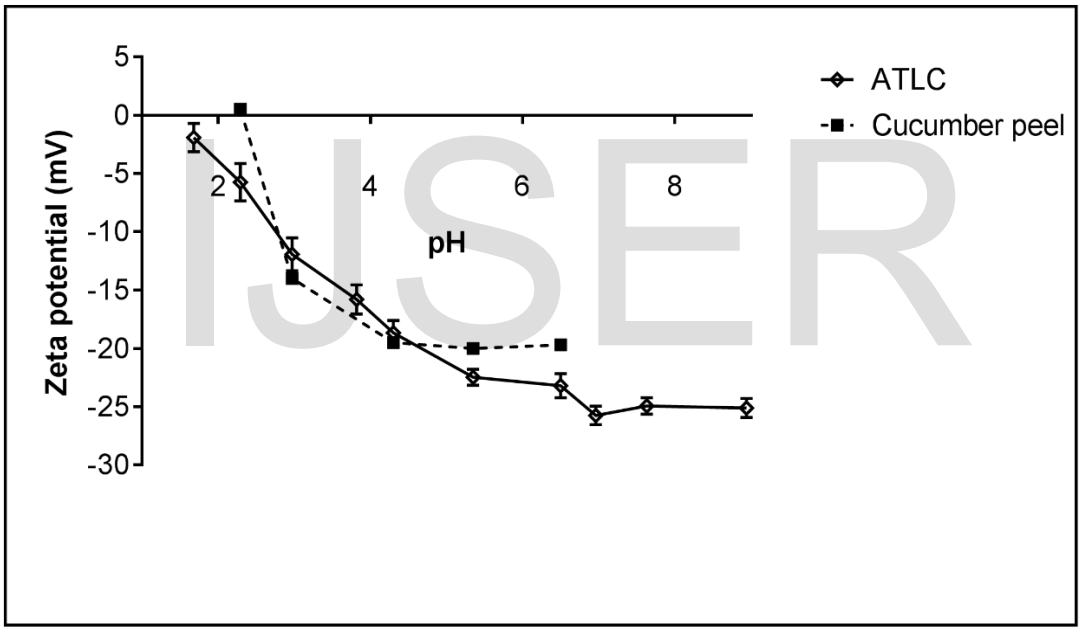

Fig. 4. The zeta potential of *ATLC* and cucumber peel at constant ionic strength in aqueous solution as a function of pH.

As compared to the chitin-lignin material of high carbon content and the grafted loofa sponge, the presence of a negative zeta potential over a pH range of 1-12 is attributed to the presence of specific functional groups, such as -COOH and -OH, on the surface which aid adsorption of metal ions [51],[53]**.** The pH at which a colloid with an acidic functional group changes from uncharged to a negative charge is related to the pK_a of those groups.

3.2 Adsorption studies as a function of acid and anion concentration onto *ATLC*.

The effect of pH on the adsorption of lead onto *ATLC* is shown in Fig 5. It can be seen that the percentage removal has a maximum at pH 5. The effect of increasing ionic strength through the addition of NaCl at a constant pH of 5 is presented in Fig 6. Interestingly the increase of chloride has minimal impact on the

uptake of Pb^{2+} onto the *ATLC* surface. Increasing NaCl up to 1 mol·L^{-1} concentration in solution supresses Pb^{2+} uptake by around 10%, with the highest extraction occurring at 0.002 mol·L^{-1} chloride.

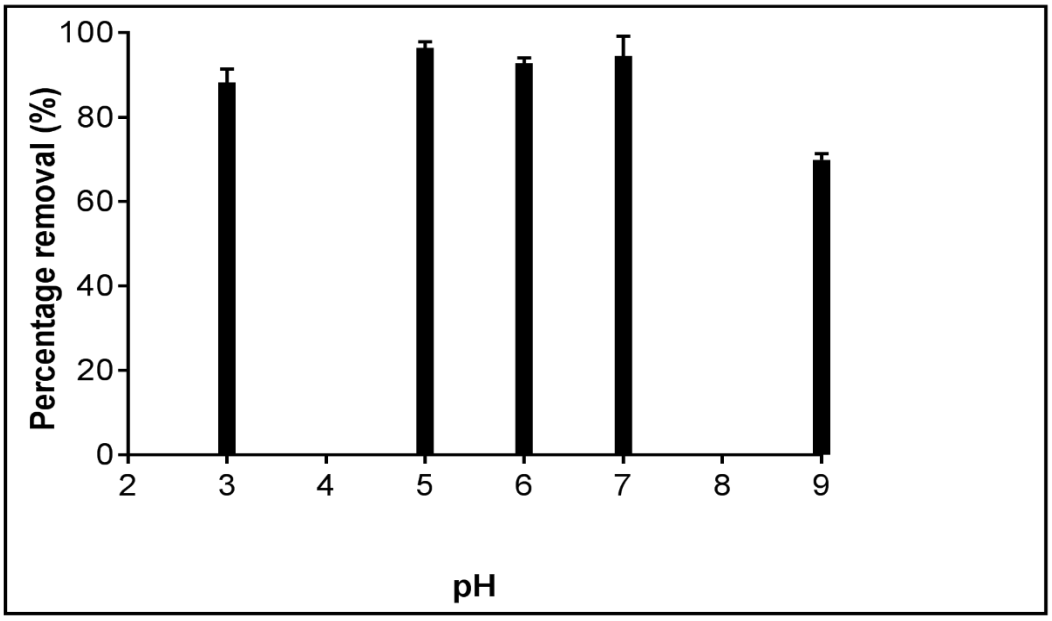

Fig. 5. Effect of solution pH conditions on the percentage removal of Pb after 24hrs contact; lead ion concentration: 50mg/L; agitation speed: 200rpm; at temperature 21°C, 5g/l biosorbent dosage.

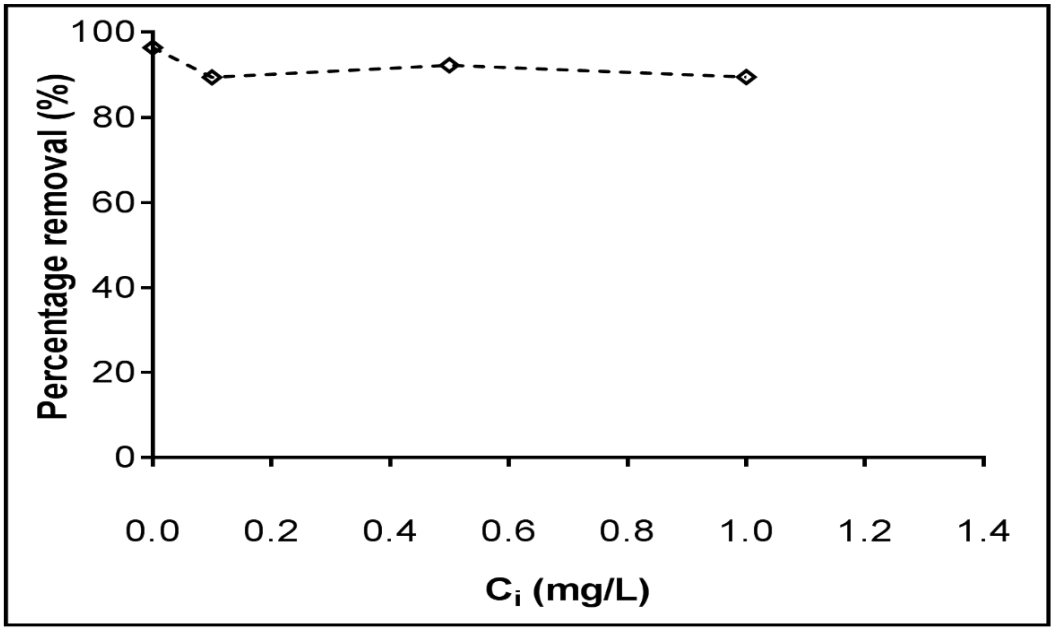

Fig. 6. Effect of chloride concentration on the percentage removal of Pb after 24 hrs contact; lead ion concentration: 50mg/L; agitation speed: 200rpm; at temperature 21^{o}C, 5g/l biosorbent dosage

pH is the most important controlling factor in the adsorption process of heavy metal ions [54]. At equilibrium pH lower than 5 the lower adsorption was attributed to the competition of H^+ ions for the binding sites on *ATLC* thereby reducing the adsorption capacity. At pHs above 6 the decrease in Pb uptake is most likely due to the hydrolysis of the metal ion in solutions. This shows the difference in lead species and their ability to be adsorbed at different solution pH. Furthermore, optimum adsorption of lead ions occurs below the point of zero charge (pH_{pzc} of 7.2). The ionic charge is positive at a lower pH and negative at a higher pH, the electrostatic attraction is opposite as the maximum uptake occurs between pH 5 – 6. Therefore, the adsorption process is dominated by ionic exchange of the ions present and other adsorption mechanisms [55]. The optimum pH for adsorption of lead ions onto tree sawdust, coconut coir and palm empty fruit bunch was similarly found to be at pH 5-6 and decreases above pH 6 [13],[57],[58],[59]. As shown in Fig 5, the lead species present at pH 5 gives 96.4% of the lead available for uptake. The potential effect of the metal ion speciation as a function of pH is presented in Fig 7 and carried out using Hyss2009 program and stability constants from the NIST database. The protonated complexes $Pb(OH)_2$, $PbOH^+$ and $Pb_3(OH)_4^{2+}$ occur in alkaline media and achieve a maximum of between 40% and 50% of hydroxylated Pb as it relates to free Pb ions. The attachment of lead ions onto the surface of loofa was highest at a pH of 5 and this indicates that the speciation of lead ions attaching are free lead ions. Furthermore, the adsorption of lead ions at over pH 7 indicates hydroxylation of the lead ions and therefore a reduction in the adsorption capacity of free lead ions to be adsorbed on the surface. The presence of free lead ions decreases as the pH increases [7],[13],[50],[52],[54],[55]. The values for the model are averages taken from low ionic strength concentrations (ClO_4^-, NO_3^- and Cl^-) from the literature.

The effect of ionic strength (Fig 6) is a dual effect of Na^+ and Cl^- ions. The tendency of Cl^- ions to form complexes with Pb^{2+} , thus decreasing the concentration of Pb^{2+} ions in solution by forming $PbCl_2$, allows for Na^+ ions to compete with remaining Pb^{2+} ions in solution for the active sites [59]. Na^+ can also occupy the active sites on *LC* limiting the binding capacity for Pb^{2+} ions [61],[55]. The binding of lead ions by *ATLC* is through both electrostatics and covalent inner and outer sphere complexes [61]. The little effect of NaCl on the Pb^{2+} ion adsorption is indicative of an inner sphere, potentially chelating, sorption mechanism [13],[31],[47]. Since, the adsorption mechanisms from the results show more than one mechanism process, the chelating adsorption indicates a fraction of the entire adsorption mechanism process is affected in the presence of ionic strength.

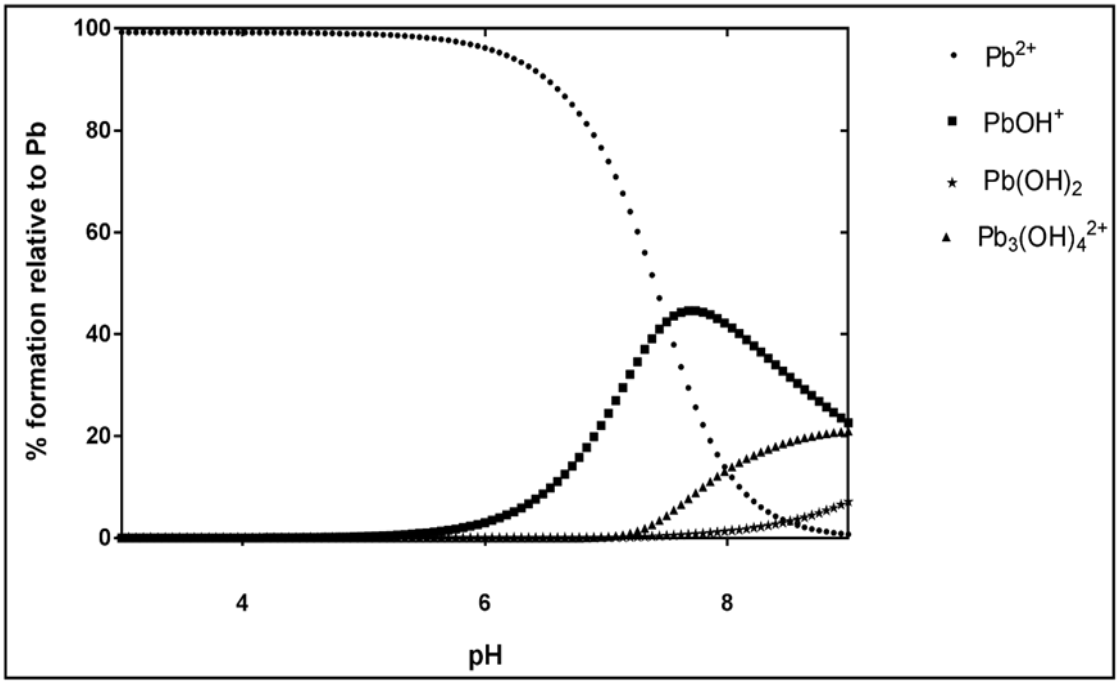

Fig. 7. Distribution of lead (II) species in aqueous solution as a function of pH.

3.3 Isotherm behaviour of removal

The isotherm fitting parameters for all the isotherm models tested is given in Table 3 based on linear regression and non-linear regression using GraphPad [20],[63]. The isotherms are used to determine the best fit in order to explain and suggest the model that best predicts the biosorption that occurs [63].

Table 3: Isotherm fitting parameter calculated using various models for lead adsorption onto *ATLC* at 21 °C and 24 hr contact time, using non-linear least squares fitting using GraphPad and SOLVER.

Langmuir		Sips	
Constant	Value	Constant	Value
K_L	0.16 ± 0.1	Ks	1.0E-01
R_L	0.09 ± 0.01	q_m	5.9 ± 0.1
q_m (mg·g^{-1})	24.9 ± 0.2	a_S	1.9 ± 0.2
R^2	0.861	R^2	0.983
Dubinin-Radushkevich		Two site Langmuir	
Constant	Value	Constant	Value
B_D (x10^{-9})	2.1 ± 0.1	K_L	0.003,1.740±0.02
q_D (mg·g^{-1})	9.6E-04	q_m (mol·g^{-1})	85.8, 12 ± 0.01
E_D (kJ·mol^{-1})	12.9 ± 0.2	R^2	0.984, 0.975
R^2	0.922		

The relationship between the equilibrium concentration and adsorption capacity is depicted in Fig 8. It shows a gradual increase in uptake capacity to a point where there is no significant change. This is a monolayer adsorption behavioural pattern. The adsorption behaviour of lead ions fitted both Langmuir, D-R and two site Langmuir models [64] but the Sips model was shown (Fig 8) to give the best fit with a R^2 value of 0.983.

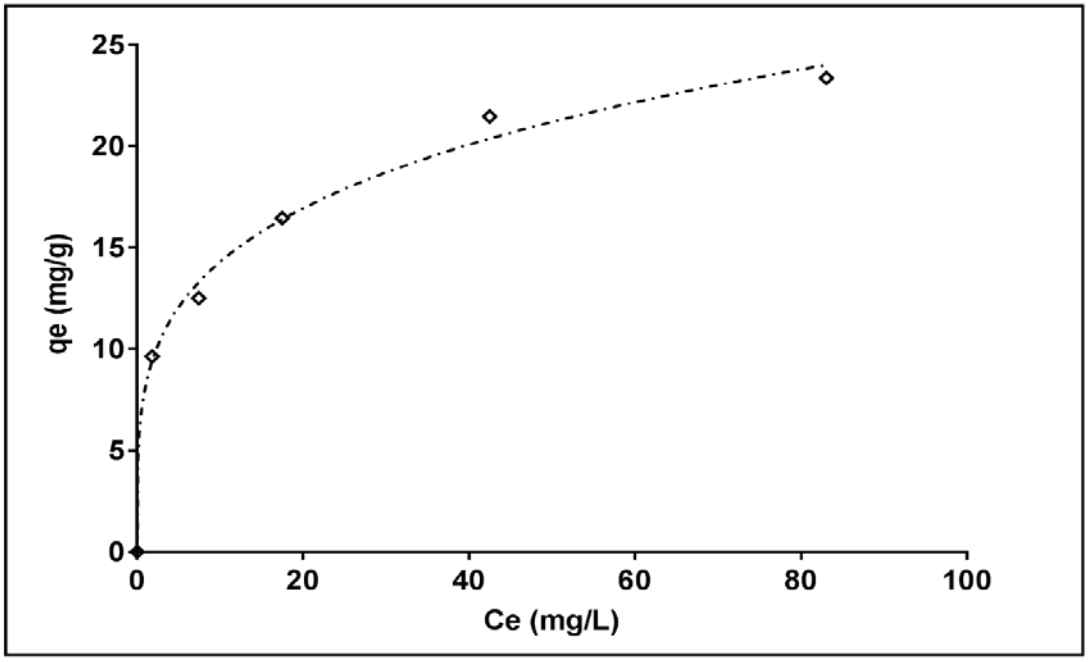

Fig. 8. Lead isotherm from pH 5.0 ± 0.1 at 21 °C and 24 hr. contact time. Sips model fit shown by dashed line.

The model fittings to Sips and two site Langmuir show a heterogeneous surfacewhich possesses both weak and strong sites. The Langmuir maximum loading capacity was 24.9 mg/g having a K_L value of 0.160L/mg. As compared to results obtained by Li *et al*. [65] which describes a Langmuir model fit, the q_{max} was lower but with a lower K_L value and according to Madala *et al*. [66], q_{max} and Langmuir constant increased as temperature increased. The K_L values relate to a higher binding energy of adsorption which leads to higher adsorption capacity [66],[67].The lead ion biosorption behaviour of *L. cylindrica* was termed a favourable adsorption. The value of 1/n at 0.245 measures the surface heterogeneity which becomes more heterogeneous with a value closer to 1 [30]. Since the E value (15.6 kJ/mol) is in the range of 8-16kJ/moles, it shows an ion exchange chemisorption process [44],[67]. However, this is taken at a lower compatibility compared to Sips model**.** The activation energy, which indicates a chemisorption mechanism with the involvement of both the surface and pores of the loofa in the adsorption process, is attributed to the presence of two different kinds of sites available for adsorption. The ion exchange capacity was calculated to be at 47%, where it accounts for every 0.0081meq of H^+ (2 moles), present on the loofa surface, 0.04959 meq of Pb^{2+} was absorbed. It further explains and supports the different mechanisms of the adsorption process that occur with the utilisation of loofa. However, the maximum loading capacity exceeds that of the ion exchange capacity, which indicates the remaining adsorption mechanism to be a surface mechanism process.

Modification of the loofa with 4% NaOH improved the adsorption capacity of lead by 9.8%. Compared to other adsorbents, such as *Luffa* charcoal, *Phanerochaete chrysosporium*, *Portulaca plant* and *Pongamia pinnata*, modified loofa (*ATLC*) shows a higher percentage removal of lead over a short period of time at room temperature. Fig 9 shows the comparison in the uptake capacity (qe(mg/g) of untreated and alkali treated loofa at pH 5 under the similar experimental conditions.

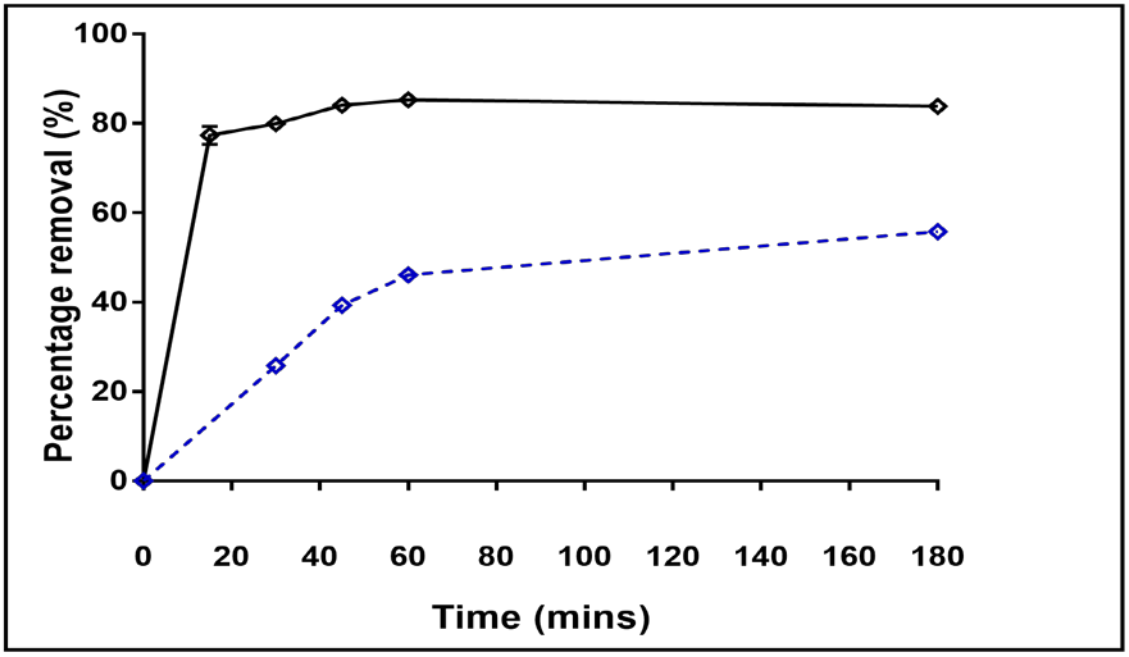

Fig. 9. Uptake capacity of lead ions with change in time for untreated and alkali treated loofa, ◆ = ATLC, ◆ = untreated LC in solution at pH 5.0 ± 0.1 at 21 °C.

Table 4: Maximum uptake capacity (isotherm model fit) of lead ions by other biosorbents between pH 5-6.

Adsorbent	q_{max} (mg/g)	Temp (°C)	Percentage removal (%)	Reference

Phanerochaete chrysosporium	12.34	27	25	[43],[44]
Pinus slyvestris	22.22	21	98	[69]
Low cost materials	4.50 – 7.56	25	99	[70]
Portulaca plant	17.24	21	78	[7]
Pongamia pinnata	34.36	30	80	[58]
Luffa acutangula	47.39	30	98	[21]
Luffa charcoal	51.02	25	80	[6]
ATLC (Luffa cylindrica)	24.90	21	96	This study

3.4 Kinetics of extraction

The modelling of batch kinetics is important in explaining the mechanism of adsorption and to determine the potential controlling steps in mass transport. The results fit the pseudo-second order (PSO) better than the pseudo first order model (Fig 10) indicating the involvement of two species in the sorption process of metal ions. As agreed with the literature, a pseudo second order model best describes the adsorption of divalent metal ions [36]. The rate constant of a pseudo second order model (k_2) increases as the concentration is increased till it reaches a peak. This shows that the uptake rate is decreased and resistance in the micropores is increased, till equilibrium is reached [71]. This may be attributed to a change in the ratio of binding interactions. The maximum adsorption capacity values of the experiments were very close in value to the model qe values as shown in table 5. Also, the fastest exchange rate, shown to occur in less than 20mins in Fig 10, may mean that exchange positions are initially on the surface**.** The increase in initial concentration results in a decrease in k_2 (K_2) and then an increase in value had been reached, a further decrease in K_2 was seen as concentration further increased. This implies that other experimental factors, not solely diffusion, play an important role in the kinetic process of adsorption. Also, this further explains the relationship between the number of available binding sites and the rate of adsorption since availability of sites is related to the initial concentration of metal ions and the time at which equilibrium adsorption capacity is reached [72].

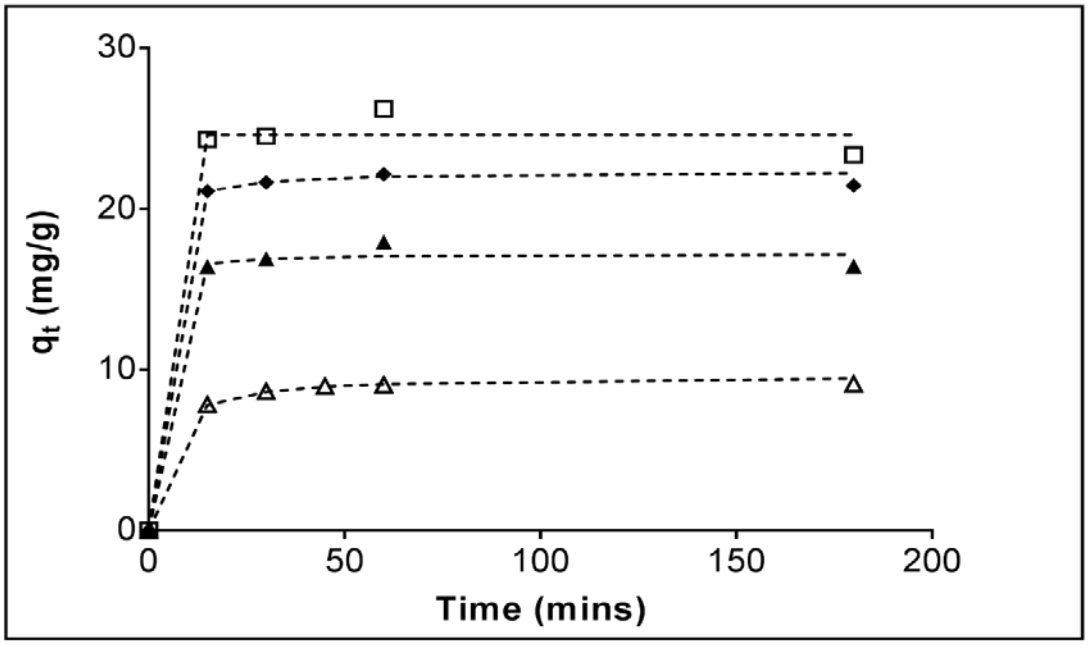

Fig. 10. Pseudo second order kinetic using non-linear regression in SOLVER(62), Δ=50mg/L, ▲=100mg/L, ◆=150mg/L, □=200mg/L Pb^{2+} in solution at pH 5.0 ± 0.1 at 21 °C. PSO model shown with dashed line.

Model efficiency, which equates to the correlation coefficient R^2 value, is a good measure to avoid errors that occur as a result of experimental values and is the best indicator for model fitting data values. The non-linear chi square test values also confirm the best fit of the model to the experiment data of the adsorption system [44],[64]. More accurate estimations are implied with smaller NSD values [73].
PSO k_2 values of 50mg/L is higher than that of 200mg/L, this shows that the sorption rate of lead ions reached a maximum value at 50mg/L, and then reduces. This indicates that the film diffusion controlling step in the mass transport process is not predominantly represented by an increase in concentration due to the involvement of other controlling mechanisms such as intra-particle diffusion, adsorbent-adsorbate interactions in solution etc. [74]. This means at higher concentration the adsorption process is not governed by film diffusion.

Table 5: Kinetic parameters of pseudo second order (Linear regression) at pH 5.7 at 21 °C

Concentration (mg/L)	q_e (mg·g^{-1})	h_0 (mins)	k_2 (g·mg^{-1}·min^{-1})
50	9.630	3.88E-03	0.062
100	16.458	0.86E-03	0.031
150	21.458	0.10E-03	0.040
200	23.359	0.26E-03	0.016

Saueprasearsit *et al*. [34] reported the use of untreated loofa for the adsorption of lead ions to be at 82.7% at a temperature of 40°C. The Langmuir model was not a good fit but it showed that the loofa surface is heterogeneous in nature by model fitting to the Freundlich model. Also, the adsorption capacity was recorded at 4.63mg/g [34],[35]. Compared to the 4% NaOH treated loofa used for this study, the percentage removal was higher (81.4% increase) and at a lower temperature which is preferable for a sustainable adsorption design process.

Table 6: Comparison of pseudo second order values obtained from lead ion (10-50mg/L) adsorption with other adsorbents.

Adsorbent	q_e (mg·g^{-1})	k_2 (g·mg^{-1}·min^{-1})	Reference
Pongamia pinnata	n/a	1.31E03	[58]
Palm kernel fiber	47.60	0.086	[44]
Portulaca plant	20.41	0.005	[7]
ATLC (Luffa cylindrica)	17.10	0.022	This study

5 Conclusions

The above results show that *L. cylindrica* is a good potential biosorbent for the removal of lead ions from aqueous solutions. Alkali treatment of *L. cylindrica* enhances the adsorption mechanism by producing additional free hydroxyl groups. The negative zeta potential shows a negatively charged loofa surface. The data show the feasibility of the modified *L. cylindrica* in the removal of lead ion from aqueous solution and also in the presence of NaCl. The change in frequency occurring due to vibrations at prominent peaks on the *L. cylindrica*, indicates the functional groups on the *L. cylindrica* that are involved in the adsorption process. The efficiency of Pb (II) uptake depicts a significant dependence on pH, metal ion concentration, temperature and ionic strength. The optimum pH of the adsorption of lead ions by *L. cylindrica* at room temperature (21^{o}C) was at pH 5-6 at equilibrium. The Sips isotherm model predicted the adsorption process better than the other models. The removal uptake of Pb (II) ions is hindered by the presence of high levels of NaCl in aqueous solution. The kinetics proved the pseudo second order model to be applicable and the adsorption rate was at 0.062g/mg/min at 50mg/L. The sorption processes of the lead ions by loofa were not solely controlled by one mechanism. The thermodynamics showed a feasible exothermic chemisorption reaction.

As compared to other recently used adsorbents in the adsorption of lead, some have been found to have a higher maximum loading capacity than loofa used in this report but because the loofa material is economically viable, widely available, requires no expensive modification of its properties, utilises no extensive technological application and can also be obtained in large quantities, it is sustainable on a global scale [76],[77].

Loofa is usually cultivated to make items such as cooking pots, bath sponges, in industrial filters and in sound insulation, it is easily grown in large quantities. The adoption of the design adsorption process with loofa will create revenue and jobs in Nigeria and also help to curb the environmental issues in the Niger Delta and other parts of the country [15],[77].

Conflict of interest

The authors declare no conflict of financial interests.

6 Acknowledgment

The authors wish to thank the Kroto Research Institute, Groundwater Protection and Restoration Group of The University of Sheffield, Andrew Fairburn, Dr. Gabriella Kakonyi, Dr. Esther Karunakaran, Dr. Joe Lovett, Separations and Nuclear Chemical Engineering Research Group, Joseph Hufton, Mat Pringle and Keith Penny. This work was supported by a grant from the Niger Delta Development Commission of the Nigerian Government (NDDC)/DEHSS award).

7 References

1. Okunola OJ, Uzairu A, Ndukwe GI, Adewusi SG. Assessment of cadmium and zinc in roadside surface soils. Res J Environ Sci. 2008;2(4):266–74.

2. Flora G, Gupta D, Tiwari A. Toxicity of lead: A review with the recent updates. Interdiscip Toxicol. 2012;5(2):47–58.
3. Islam E, Liu D, Li T, Yang X, Jin X, Mahmood Q. Effect of Pb toxicity on leaf growth, physiology and ultrastructure in the two ecotypes of Elsholtzia argyi. J Hazard Mater. 2008;154(1–3):914–26.
4. Andra SS, Datta R, Sarkar D, Makris KC, Mullens CP, Sahi S V. Induction of lead-binding phytochelatins in vetiver grass Vetiveria zizanioides (L.). J Environ Qual. 2008;38(3):868–77.
5. Punamiya P, Datta R, Sarkar D, Barber S, Patel M, D P. Symbiotic role of Glomus mosseae in phytoextraction of lead in vetiver grass [Chrysopogon zizanioides (L.)]. Journal of Hazardous Materials. 2010;177(1–3):465–74.
6. Umpuch C, Bunmanan U, Kueasing U, Kaewsan P, Bunmanan N, Kueasing U. Adsorption of lead from synthetic solution using luffa charcoal. World Acad Sci Eng Technol. 2011;5(09):24.
7. Dubey, A.Shiwani S, Dubey A, Shiwani S. Adsorption of lead using a new green material obtained from Portulaca plant. Int J Environental Sci Technol. 2012;9:15–20.
8. Olawale AM. Bioremediation of wastewater from an industrial effluent system in Nigeria using Pseudomonas aeruginosa: Effectiveness tested on albino rats. J Pet Environ Biotechnol. 2014;5(1):1–4.
9. Ayenimo JG, Adeeyinwo CE, Amoo IA. Heavy metal pollutants in Warri river, Nigeria. Kragujev J Sci. 2005;27:43–50.
10. Anyakora C, Nwaeze K, Awodele O, Nwadike C, Arbabi M, Coker H. Concentrations of heavy metals in some pharmaceutical effluents in Lagos, Nigeria. J Environ Chem Ecotoxicol. 2011;3(2):25–31.
11. Pourrut B, Shahid M, Dumat C, Winterton P, Pinelli E. Lead uptake, toxicity, and detoxitication in plants. Rev Environ Contam Toxicol. 2011;213:113–36.
12. Adewumi and Oguntuase, Adewumi JR, Oguntuase AM. Planning of wastewater reuse programme in Nigeria. J Sustain Dvelopment. 2016;15(1):1–33.
13. Sangi MR, Shahmoradi A, Zolgharnein J, Azimi GH, Ghorbandoost M. Removal and recovery of heavy metals from aqueous solution using Ulmus carpinifolia and Fraxinus excelsior tree leaves. J Hazard Mater. 2008;155(3):513–22.
14. Ali I, Asim M, Khan T A. Low cost adsorbents for the removal of organic pollutants from wastewater. J Environ Management; 2012 Dec 30;113:170–83.
15. Ajuru M, Nmom F. A Review on the Economic Uses of Species of Cucurbitaceae and Their Sustainability in Nigeria. Am J Plant Biol. 2017;2(1):17–24.
16. Laidani Y, Hanini S, Mortha G, Heninia G. Study of fibrous annual plant, luffa cylindrica for paper application .Part I: Charatcerization of the vegetal. Iran J Chem Chem Eng. 2012;31(4):119–29.
17. Chen Q, Shi Q, Gorb SN, Li Z. A multiscale study on the structural and mechanical properties of the Luffa cylindrica plant. J Biomech. 2014;47(6):1332–9.
18. Siqueira G, Bras J, Dufresne A. Luffa cylindrica as a lignocellulosic source of fiber, microfibrillated cellulose, and cellulose nanocrystals. 2010;5:727–40.
19. Iqbal M, Edyvean RGJ. Biosorption of lead, copper and zinc ions on loofa sponge immobilized biomass of Phanerochaete chrysosporium. Miner Eng. 2004;17(2):217–23.
20. Benhima H, Chiban M, Sinan F, Seta P, Persin M. Removal of lead and cadmium ions from aqueous solution by adsorption onto micro-particles of dry plants. Colloids Surf B Biointerfaces. 2008;61(1):10–6.
21. Boudechiche N, Mokaddem H, Sadaoui Z, Trari M. Biosorption of cationic dye from aqueous soutions onto lignocellulosic biomass (Luffa cylindrica): charcaterisation, equilibrium, kinetic and thermodynamic studies. Int J Ind Chem. 2016;7(2):167–80.
22. Suhas, Gupta VK, Carrott PJM, Singh R, Chaudhary M, Kushwaha S. Cellulose: A review as natural, modified and activated carbon adsorbent. Vol. 216, Bioresource Technology. 2016.
23. Akhtar N, Iqbal J, Iqbal M. Microalgal-luffa sponge immobilized disc: a new efficient biosorbent for the removal of Ni(II) from aqueous solution. Lett Appl Microbiol. 2003;37(Ii):149–53.

24. Oboh IO, Aluyor EO. Luffa cylindrica. 2009;4(August):684–8.
25. Yukselen Y, Kaya A. Zeta Potential of Kaolinite in the Presences of Alkali, Alkaline Earth and Hydrolyzable Metal ions. Water Air Soil Pollut. 2003;
26. Kim J, Lawler DF. Charactersitics of Zeta Potential Distribution in Silica Particles. Bull Korean Chem Soc. 2005;26(7):1083–9.
27. Harland CE. Ion exchange: Theory and Practice. 1994. 137-141.
28. Chen X. Modeling of Experimental Adsorption Isotherm Data. Information. 2015;6(1):14–22.
29. Ozkaya B, Özkaya B. Adsorption and desorption of phenol on activated carbon and a comparison of isotherm models. J Hazard Mater. 2006;129(1–3):158–63.
30. Foo KYY, Hameed BHH. Insights into the modeling of adsorption isotherm systems. Chem Eng J. 2010;156(1):2–10.
31. Yang B, Zuo J, Tang XX, Liu F, Yu X, Tang XX. Effective ultrasound electrochemical degradation of methylene blue wastewater using a nanocoated electrode. Ultrason Sonochem. Elsevier B.V.; 2014 Jul;21(4):1310–7.
32. Nong G, Zhou Z, Wang S. Generation of hydrogen, lignin and sodium hydroxide from pulping black liquor by electrolysis. Energies. 2016;9(1).
33. Ghali L, Msahli S, Zidi M, Sakli F. Effect of pre-treatment of Luffa fibres on the structural properties. Mater Lett. Elsevier B.V.; 2009;63(1):61–3.
34. Saueprasearsit P, Nuanjaraen M, Chinlapa M. Biosorption of Lead (Pb2+) by Luffa cylindrica Fiber. Environ Res J. 2010;4(1):157–66.
35. Tang WW, Zeng GM, Gong JL, Liang J, Xu P, Zhang C. Impact of humic/fulvic acid on the removal of heavy metals from aqueous solutions using nanomaterials: A review. Sci Total Environ. Elsevier B.V.; 2014;468–469:1014–27.
36. Vilar VJP, Botelho CMS, Pinheiro JPS, Domingos RF, Boaventura R a R. Copper removal by algal biomass: Biosorbents characterization and equilibrium modelling. J Hazard Mater. 2009 Apr 30;163(2–3):1113–22.
37. Lasheen MR, Ammar NS, Ibrahim HS. Adsorption/desorption of Cd(II), Cu(II) and Pb(II) using chemically modified orange peel: Equilibrium and kinetic studies. Solid State Sci. Elsevier Masson SAS; 2012;14(2):202–10.
38. Rodriguez Correa C, Otto T, Kruse A. Influence of the biomass components on the pore formation of activated carbon. Biomass and Bioenergy. 2017;97(Supplement C):53–64.
39. Hassan M. Quaternization and anion exchange capacity of sponge gourd (Luffa cylindrica). Appl Polym. 2006;101(4):2495–503.
40. Bai RS, Abraham TE. Studies on enhancement of Cr(VI) biosorption by chemically modified biomass of Rhizopus nigricans. Water Res. 2002;36(5):1224–36.
41. Williams D, Fleming I, Dudley, Williams FI. Spectroscopic methods in organic chemistry. 2008;
42. Whittaker D. Interpreting organic spectra. R Soc Chem. 2000;
43. Jayamani E, Hamdan S, Heng SK, Rahman MR, Bakri MK, Kakar A. The Effect of Natural Fibres Mercerization on Natural Fibres/Polypropylene Composites: A Study of Thermal Stability, Morphology and Infrared Spectrum. Aust J Basic Appl Sci. 2014;8(1991–8178):332–40.
44. Shaikh T, Agrawal SA. Qualitative and Quantitative Characterization of Textile Material by Fourier Transform Infra-Red. Int J Innov Res Sci Eng Technol. 2014;3(1).
45. Anastopoulos I, Massas I, Ehaliotis C. Composting improves biosorption of Pb2+and Ni2+ by renewable lignocellulosic materials. Characteristics and mechanisms involved. Chem Eng J. Elsevier B.V.; 2013;231:245–54.
46. Saw SK, Purwar R, Nandy S, Ghose J, Sarkhel G. Fabrication, characterisation ad evaluation of Luffa cylindrica fiber reinforced epoxy composites. Bioresources. 2013;8(4).
47. OuYang X, Yang L, Wen Z. Adsorption of Pb(II) from solution using peanut shell as biosorbent in the presence of amino acid and sodium chloride. Bioresources. 2014;9(2).
48. Stana-Kleinschek K, Ribitsch V, Kreze T, Lidija F, Fras L. Determination of the adsorption character of cellulose fibres using surface tension and surface charge. Mater Res Innov.

2002;6(1):13–8.

49. Basu M, Guha AK, Ray L. Adsorption of Lead on Cucumber Peel. J Clean Prod. Elsevier Ltd; 2017;151(Supplement C):603–15.
50. Wu S, Zhao X, Li Y, Du Q, Sun J, Wang Y. Adsorption properties of doxorubicin hydrochloride onto graphene oxide: Equilibrium, kinetic and thermodynamic studies. Materials (Basel). 2013;6(5):2026–42.
51. Zdarta J, Klapiszewski Ł, Wysokowski M, Norman M, Kołodziejczak-Radzimska A, Moszyński D. Chitin-lignin material as a novel matrix for enzyme immobilization. Mar Drugs. 2015;13(4):2424–46.
52. Adewuyi A, Vargas F. Isolation and surface modification of cellulose from underutilized Luffa cylindrica sponge : A potential feed stock for local polymer industry in Africa. J Assoc Arab Univ Basic Appl Sci. University of Bahrain; 2017;24:39–45.
53. Liu C, Yan C, Zhou S, Ge W. Fabrication of sponge biomass adsorbent through UV-induced surface-initiated polymerization for the adsorption of Ce(II) from wastewater. Water Sci Technol. 2017;75(12):2755–64.
54. Saeed A, Iqbal M, Zafar SI, Iqbal S. Immobilization of Trichoderma viride for enhanced methylene blue biosorption: Batch and column studies. J Hazard Mater. 2009;168(1):406–15.
55. Iqbal M, Saeed A, Zafar SI, Iqbal S. FTIR spectrophotometry, kinetics and adsorption isotherms modeling, ion exchange, and EDX analysis for understanding the mechanism of Cd2+ and Pb2+ removal by mango peel waste. J Hazard Mater. 2009;164(1):161–71.
56. Feng N, Guo X, Liang S, Zhu Y, Liu J. Biosorption of heavy metals from aqueous solutions by chemically modified orange peel. J Hazard Mater. Elsevier B.V.; 2011;185(1):49–54.
57. Ahmad R, Haseeb S. Kinetic, isotherm and thermodynamic studies for the removal of lead ion by a novel adsorbent Luffa acutangula (LAPR). Desalin Water Treat. 2015;
58. Yusoff SNM, Kamari A, Putra WP, Ishak CF, Mohamed A, Hashim N. Removal of Cu(II), Pb(II0 and Zn(II) ions from aqueous solutions using selected agricultural wastes: Adsorption and characterisation studies. J Environ Prot (Irvine, Calif). 2014;5:289–300.
59. Volesky B. Sorption and Biosorption. 2003;
60. Arshadi M, Amiri MJ, Mousavi S. Kinetic , equilibrium and thermodynamic investigations of Ni (II), Cd (II), Cu (II) and Co (II) adsorption on barley straw ash. Water Resour Ind. Elsevier; 2014;6:1–17.
61. Holmberg JP. Competitive adsorption and displacement behaviour of heavy metals on peat. 2006;
62. Hossain MA, Ngo HH, Guo W, Hossain A, Ngo HH, Guo W. Introductory of Microsoft Excel SOLVER Function - Spreadsheet Method for Isotherm and Kinetics Modelling of Metals Biosorption in Water and Wastewater. J Water Sustain. 2013;3(4):223–37.
63. Oboh I, Aluyor E, Audu T. Biosorption of heavy metal ions from aqueous solutions using a biomaterial. Leonardo J Sci. 2009;(14):58–65.
64. Dada A., Olalekan AP, Olatunya AM, Dada O. Langmuir , Freundlich , Temkin and Dubinin – Radushkevich Isotherms Studies of Equilibrium Sorption of Zn 2 + Unto Phosphoric Acid Modified Rice Husk. 2012;3(1):38–45.
65. Li X, Liao D, Xu X, Yang Q, Zeng G, Zheng W Kinetic studies for the biosorption of lead and copper ions by Penicillium simplicissimum immobilized within loofa sponge. J Hazard Mater. 2008;159(2–3):610–5.
66. Madala S, Nadavala SK, Vudagandla S, Boddu VM, Abburi K. Equilibrium, kinetics and thermodynamics of Cadmium (II) biosorption on to composite chitosan biosorbent. Arab J Chem. King Saud University; 2013 Jul;
67. Mamatha M, Aravinda HB, Manjappa S, Puttaiah ET. Kinetics and mechanism for adsorption of lead in aqueous and industrial effluent from Pongamia pinnata tree bark. J Environ Sci. 2012;2(2):1–9.
68. Shaikh T, Agrawal S and. Qualitative and Quantitative Characterization of Textile Material by

Fourier Transform Infra-Red. Int J Innov Res Sci Eng Technol. 2014;3(1):8496–502.

69. Taty-Costodes VC, Fauduet H, Porte C, Delacroix A. Removal of Cd(II) and Pb(II) ions, from aqueous solutions, by adsorption onto sawdust of Pinus sylvestris. J Hazard Mater. 2003;105(1–3):121–42.
70. Mishra PC, Patel RK. Removal of lead and zinc ions from water by low cost adsorbents. J Hazard Mater. 2009 Aug 30;168(1):319–25.
71. Yu J, Wang L, Chi R, Zhang Y, Xu Z, Guo J. Removal of cationic dyes: basic magneta and methylene blue from aqueous solution by adsorption on modified loofah. Res Chem Intermed. 39(8).
72. Plazinski W, Rudzinski W, Plazinska A. Theoretical models of sorption kinetics including a surface reaction mechanism: A review. Adv Colloid Interface Sci. Elsevier B.V.; 2009;152(1–2):2–13.
73. Gholizadeh A, Kermani M, Gholami M, Farzadkia M. Kinetic and isotherm studies of adsorption and biosorption process in the removal of phenolic compounds from aqueous solutions : comparative study. J Environ Heal Sci Eng. 2013;11(29).
74. Kumar A, Jena HM. Removal of methylene blue and phenol onto prepared activated carbon from Fox nutshell by chemical actiavtion in batch and fixed -bed column. J Clean Prod. 2016;137:1246–59.
75. Barakat M a. New trends in removing heavy metals from industrial wastewater. Arab J Chem. King Saud University; 2011 Oct;4(4):361–77.
76. Tsibranska I, Hristova E, Tsibranka I, Hristova E. Comparison of different kinetic models for adsorption of heavy metals onton activated carbon from apricot stones. Bulg Chem Commun. 2011;43(3):370–7.
77. Agbabiaka LA, Okorie KC, Ezeafulukwe CF. Plantain peels as dietary supplement in pratical diest for African catfish (Clarias gariepinus burchell 1822) fingerlings. Agric Biol J North Am. 2013;

Authors' Information

Akanimo U. Emene[1], Robert Edyvean[1]

[1]Department of Chemical and Biological Engineering, University of Sheffield, Western Bank, Sheffield, S10 2TN, United Kingdom

Corresponding author email: a.emene-amba@sheffield.ac.uk